

## 2.D X-Ray Crystal Devices: Diagnostic Developments

Laser-fusion experiments will involve ever-increasing compressed target densities, attained in regions of small spatial dimension. With fast-electron preheat minimized by the use of short-wavelength laser radiation, ablatively driven targets are expected to produce high-density imploded cores at relatively low temperatures. For diagnostic purposes, there is a clear need for x-ray devices of greater sensitivity and higher spatial resolution.

We report here three developments in x-ray diagnostics: (a) using a Von-Hamos x-ray spectrograph, we have obtained ionic spectral lines of higher energy (12–14 keV) than has been previously observed; (b) mosaic crystals have been used in a geometry which yields both high sensitivity and resolution; and (c) two-dimensional imaging of  $\sim 10\text{-}\mu\text{m}$  resolution has been achieved using Laue diffraction.

### Von-Hamos Focusing Crystal Spectrography

The Von-Hamos x-ray spectrograph<sup>1</sup> consists of a cylindrically curved crystal whose axis normally lies in the plane of the recording film. The radiation source lies on this axis as well (see Fig. 11a). A wide-range spectrum is obtained on the film with a flux which is higher by a large factor than in the corresponding flat-crystal case. This factor, of the order of the ratio between the crystal radius of curvature and the source radius, can be several hundred for laser-fusion targets. In a preliminary study,<sup>1</sup> we demonstrated an increase by a factor  $>100$  in the flux on film, by bending mica to a 5-cm radius of curvature and observing first-order diffraction of radiation from laser-irradiated targets. This increase in sensitivity is important for the diagnosis of high-density, low-temperature implosions. To realize the full potential of the instrument it is crucial to master the art of bending crystals to small radii of curvature. Considerable effort has been devoted to studying the properties of various crystals under bending, polishing, and abrading treatments; this is reported elsewhere.<sup>2</sup>

Figure 11 shows an example of focusing (imaging) using a mica crystal in fifth order. The source (Fig. 11b) was a steel mesh (50- $\mu\text{m}$  bar width) fluorescing Fe  $K_{\alpha}$  radiation when irradiated by copper  $K_{\alpha}$  radiation from an x-ray tube. Spatial resolution of at least 50  $\mu\text{m}$  is evident in Fig. 11c. Imaging in the up-down direction in the plane of Fig. 11c is entirely due to the Von-Hamos focusing. Imaging in the left-right, dispersion direction is due to the monochromaticity of the radiation source.

In order to demonstrate further the capabilities of the Von-Hamos spectrometer, we performed a small number of test shots on the 24-beam OMEGA laser system. In these shots, short pulses (100 ps) of high power ( $\sim 6$  TW) were used to explosively implode small targets (diameters 50–80  $\mu\text{m}$ ), in which high core temperatures of 3–4 keV were achieved. The unique capability of

the instrument is demonstrated by the observation of spectral lines from the compressed core of a shorter wavelength ( $0.95 \text{ \AA}$ ) than any previously reported ionic lines (see Fig. 12). Furthermore, all spectra were so intense as to cause film saturation. We stripped the front emulsion of the (Kodak no-screen) film by a bleaching agent and the spectra shown in Fig. 12 were recorded on the back emulsion, being very intense even then.

These spectra were obtained with two curved crystals: LiF 200 ( $2d = 4.03 \text{ \AA}$ ) and LiF 220 ( $2d = 2.85 \text{ \AA}$ ). The Ge spectrum was obtained from imploding germania ( $\text{GeO}_2$ ) shells of diameter  $50 \mu\text{m}$  and thickness  $0.7 \mu\text{m}$ . The Kr lines were obtained from a glass shell of diameter  $57 \mu\text{m}$  and wall thickness  $1.05 \mu\text{m}$ , filled with krypton at a pressure of 10 atm. To observe the higher-energy lines of the  $\text{Kr}^{+34}$  spectrum, a different crystal would be required.

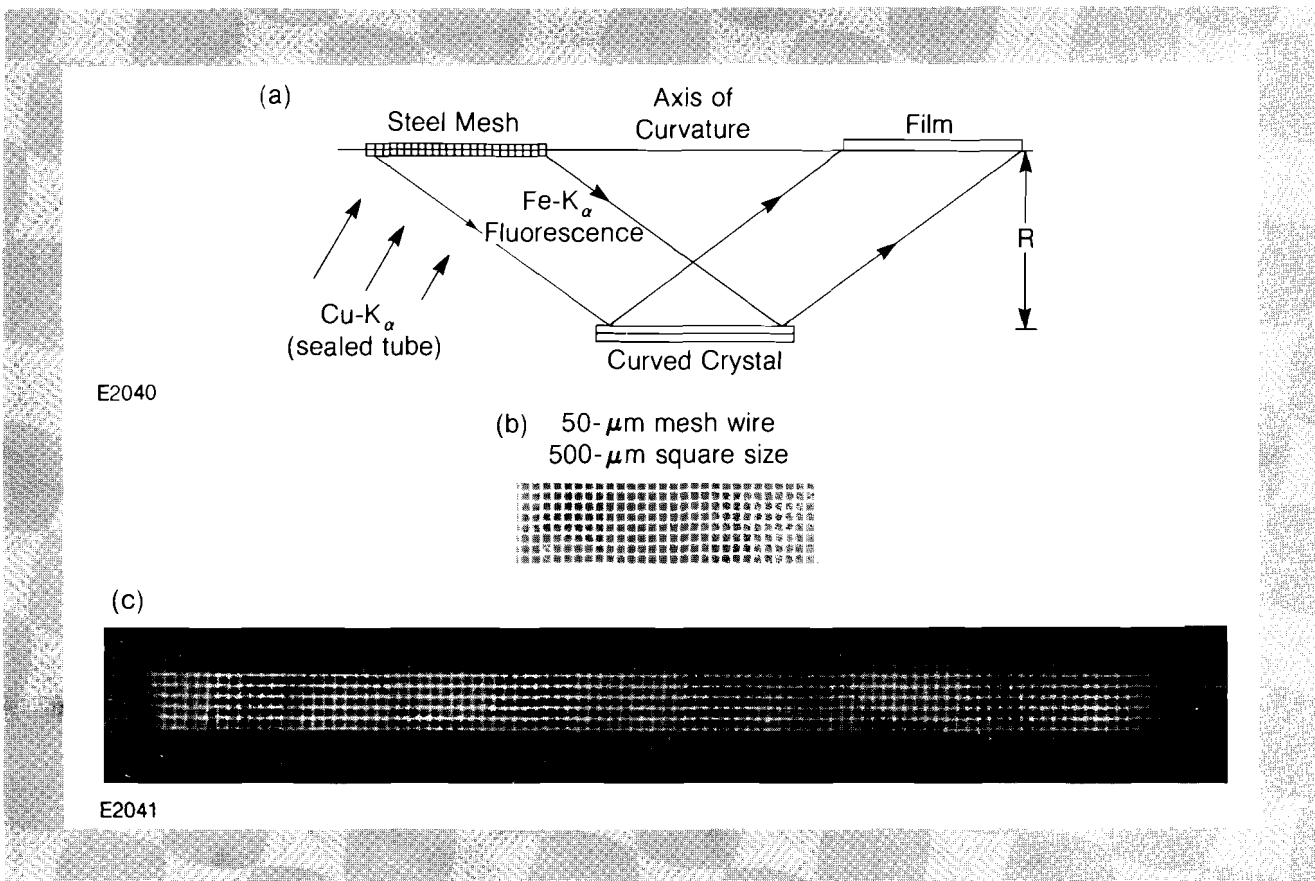


Fig. 11

- a): Von-Hamos configuration. The x-ray source (a stainless-steel mesh used to produce  $\text{Fe K}_\alpha$  radiation) and the film are placed on the axis of curvature of the mica crystal. The flux on the film is considerably enhanced by the curvature of the crystal.
- b): Segment of mesh used as test-pattern.
- c): Image of test pattern obtained with Von-Hamos spectrometer: imaging in the up-down direction is due to Von-Hamos focusing, and imaging in the left-right (dispersion) direction is due to the monochromaticity of the source.

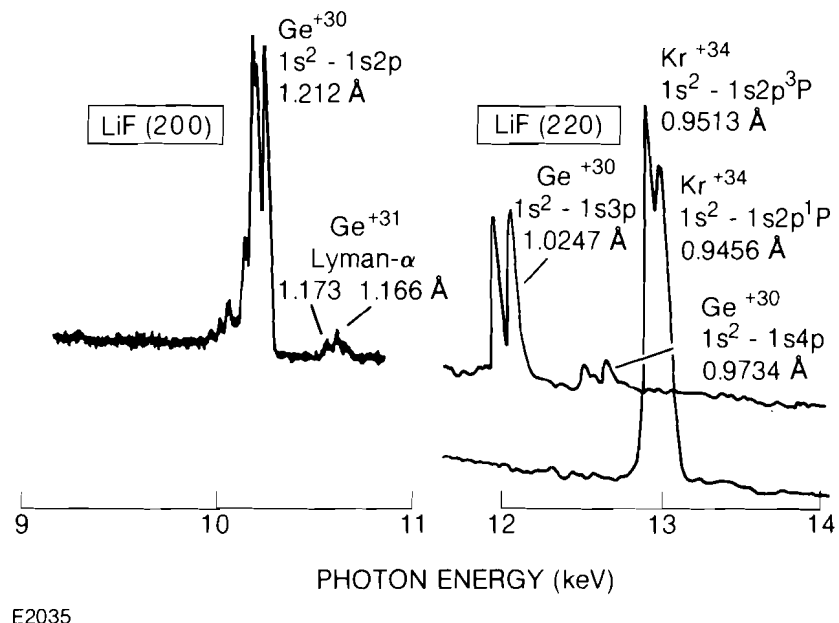


Fig. 12

Spectra obtained by curved LiF (200) and LiF (220) crystals. Ge lines are from Germania ( $\text{GeO}_2$ ) shells, Kr lines from krypton-filled glass shells.

### Mosaic Focusing

Mosaic focusing arises from the little-noticed fact that x rays from a monochromatic point source reflected off a mosaic crystal converge to a point of equal distance from the crystal as the source, before diverging away (see Fig. 13). Normally, mosaic crystals are considered to be high-sensitivity, low-resolution diffracting devices. However, recording at the focal position described above, a mosaic crystal simultaneously provides high resolution and sensitivity.

Mosaic focusing is demonstrated by comparing Figs. 14 and 15. In each case the upper spectrum is obtained from a flat pyrolytic-graphite crystal (002), which is highly mosaic with a mosaic spread of about  $0.8^\circ$ ; the lower comparison spectra are recorded by a flat Ge (111) crystal. The experimental conditions in these two figures are very different; however, the pairs of spectra in each figure correspond to the same laser conditions and the same geometry of the measuring device.

In Fig. 14, the focusing conditions are not met, whereas in Fig. 15 they are. The mosaic focusing is dramatically evident in Fig. 15 where the highly mosaic graphite crystal is shown to have adequate spectral resolution for laser-fusion applications. Moreover, graphite in the focusing geometry retains a higher reflectivity than Ge (111), by a factor which varies in the range of 10–15 over the spectrum. In fact, to obtain the spectra of Fig. 15, we had to use severe attenuation ( $\sim 4\times$ ) to prevent the spectrum produced by the graphite from saturating the film. The fluctuations in the background level are probably due to large-scale crystal inhomogeneities.

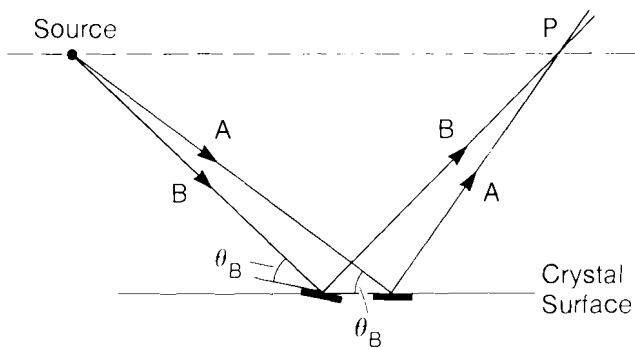
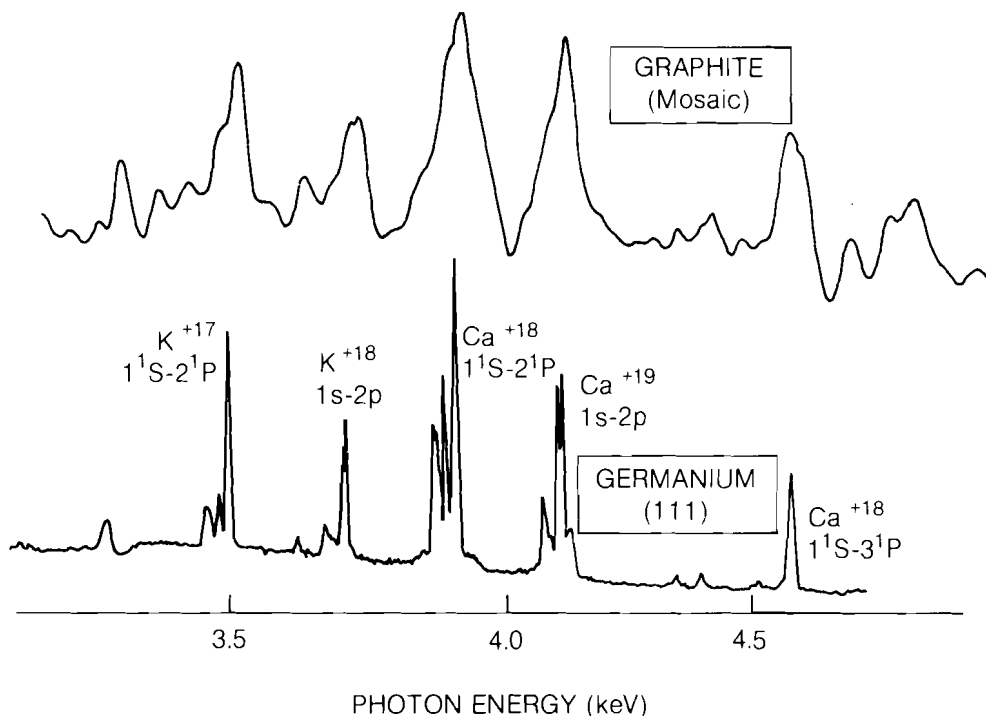


Fig. 13  
Focusing from a mosaic crystal. X rays (A) and (B) Bragg-reflect off crystal segments misaligned by small angles from the average crystal plane. Both rays pass through the point P, at which an enhanced x-ray flux will be obtained.



E2292

Fig. 14  
Effect of mosaic spread in a non-focusing geometry. X-ray spectra from glass impurities are measured simultaneously by a pyrolytic-graphite (002) crystal with 0.8° mosaic spread and a Ge (111) crystal. Laser: ZETA six-beam system,  $\lambda = 1.05 \mu m$ , 108 J in 73 ps. Target: glass microballoon, diameter 50  $\mu m$ , thickness 2.2  $\mu m$ .

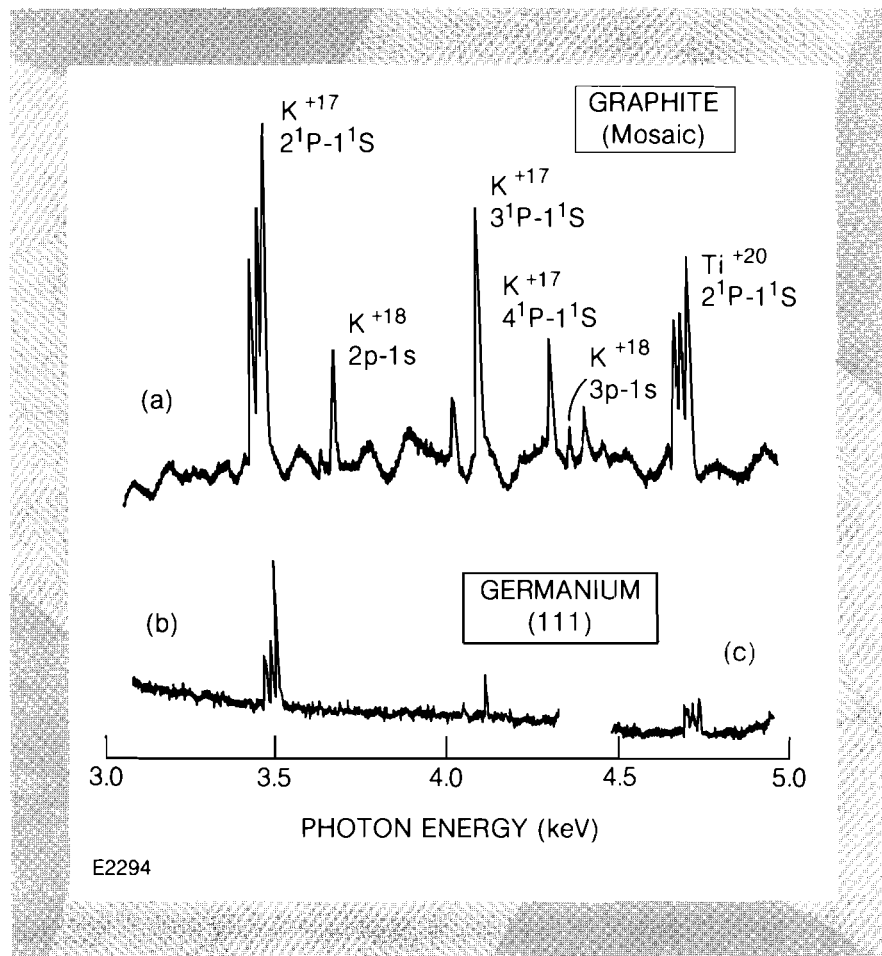


Fig. 15

Demonstration of mosaic focusing. Graphite (002) and Ge (111) crystals are both placed in the focusing geometry of Fig. 13. Spectra in (a) and (b) were attenuated by a 190- $\mu\text{m}$ -thick mylar foil to prevent film saturation by the radiation diffracted off the graphite. In (c) only a 95- $\mu\text{m}$ -thick mylar foil was employed. The density scale of (b) and (c) was expanded by a factor of 2 to make the traces for the two crystals have more comparable heights.

#### Achromatic Imaging with Laue Crystal Diffraction

The Laue crystal geometry for x-ray crystal diffraction was described in an earlier issue of the LLE Review.<sup>3</sup> When used in the configuration indicated in Fig. 16, with the film placed at the focus, two-dimensional (achromatic) resolution can be achieved. Imaging in the up-down direction in the plane of the figure is due to the focusing character of Laue diffraction and is of unit magnification. Imaging in the direction perpendicular to the plane of the figure may be obtained either by placing a slit anywhere between the source and the film, or by backlighting the object with a narrow line source. The long dimension of the slit (or the line source) lies in the plane of the figure.

The spatial resolution is limited by the broadening of the beam in traversing the crystal, because of repeated diffraction from successive crystal planes. Clearly it is necessary to etch the crystal down to a small thickness. For thin crystals, the spatial resolution is limited by the angular width of the diffraction rocking curve, which increases when the crystal becomes thinner. For example, for the  $\text{Ti}^{+20}$  resonance line at 2.62  $\text{\AA}$ , a Ge (111) or Si (111) crystal etched down to a 20- $\mu\text{m}$  thickness can achieve a resolution of about 17  $\mu\text{m}$ . Recent developments in the semiconductor industry (such as boron implantation) can be used to

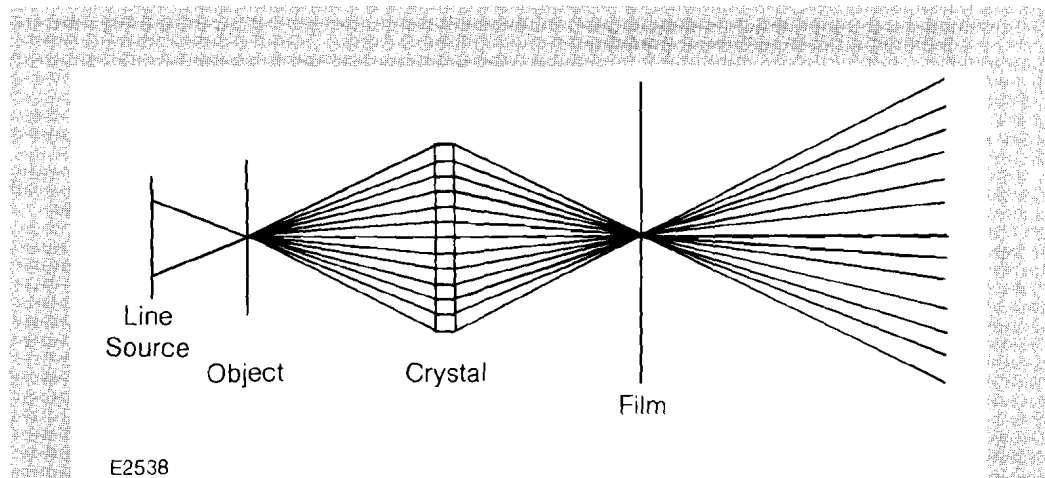


*Fig. 16*  
Schematic of Laue diffraction geometry. When the film is placed at the focus as indicated, spatial resolution is obtained at the expense of spectral resolution.

fabricate crystals as thin as a few microns. Planar etching can also be used to fabricate such crystals.

In order to demonstrate the two-dimensional imaging capability of the Laue geometry, we used a 3.75- $\mu\text{m}$ -thick Germanium crystal with the (111) Laue diffracting planes. The object was a gold wire mesh, with a fine mesh of 10- $\mu\text{m}$ -thick wire supported on a coarse mesh of 50- $\mu\text{m}$ -thick wire. The mesh and the film were placed at the two conjugate points of the Laue crystal (each 8.4 cm from the crystal) and the mesh was backlit by a Cr x-ray tube ( $\lambda = 2.3 \text{ \AA}$ ). The x-ray tube was positioned so as to project a line focus about 1 cm wide in the direction of dispersion and several microns high. Because of the narrow height of the foreshortened source there was no need for a spatially resolving slit. The image obtained with this setup is shown in Fig. 17, where a resolution of less than 10  $\mu\text{m}$  (in both dimensions) is evident.

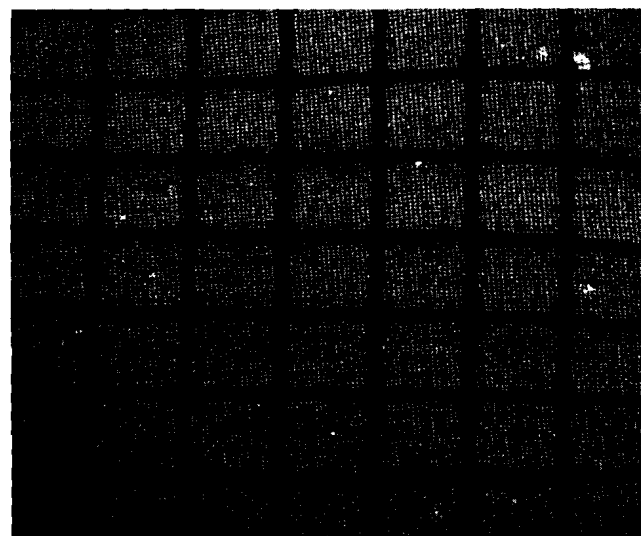


*Fig. 17*  
Two-dimensional achromatic Laue image of a test pattern comprising a 10- $\mu\text{m}$ -thick gold wire mesh placed over a 50- $\mu\text{m}$ -thick wire mesh. Crystal: 3.75- $\mu\text{m}$ -thick Ge (111). Source: Cr x-ray tube (2.3  $\text{\AA}$ ). Dispersion is in the left-right direction.

E2313

→||← 50  $\mu\text{m}$

This result demonstrates that Laue crystal diffraction can be a useful diagnostic technique for laser-plasma experiments such as backlighting.

REFERENCES

1. B. Yaakobi, R. E. Turner, H. W. Schnopper, and P. O. Taylor, *Rev. Sci. Instrum.* **50**, 1609 (1979).
2. B. Yaakobi and A. J. Burek, LLE Report 139, 1983 (unpublished).
3. LLE Review **11**, 34 (1982).